Accident Analysis and Prevention 233 (2026) 108574

Contents lists available at ScienceDirect

Accident Analysis and Prevention

journal homepage: www.elsevier.com/locate/aap

Towards self-explaining spiral tunnels: road-prototype-based facility design and visual-perception fluid assessment

Yanzi Xia [a], Chi Zhang [a,*], Min Zhang [b], Bo Wang [a], Yanyang Gao [a], Sheng Xu [c]

[a] School of Highway, Chang'an University, Xi'an 710064, China
[b] School of Transportation Engineering, Chang'an University, Xi'an 710064, China
[c] School of Economics and Management, Chang'an University, Xi'an 710064, China

ARTICLE INFO

Keywords:
Self-explaining road
Spiral tunnels
Visual-perception fluid
Road prototype design
Environmental semantic segmentation

ABSTRACT

With increasing demand for spiral tunnels, drivers face spatial cognitive challenges due to strong geometry transitions. To address this issue, a self-explaining-road-based framework is developed, focusing on the system-level optimization of four categories of tunnel environmental facilities, including visual guidance facilities, traffic signs, overall environment, and roadway. These elements are systematically combined under a road prototype design approach to induce expected driving behavior. In addition, a visual-perception fluid (VPF) model is proposed to evaluate drivers' visual-perception performance in spiral tunnels. Four semantic categories were extracted via environmental semantic segmentation to compute equivalence mass of environmental information, information flow velocity, cognitive resistance, and composite VPF index. A driving-simulator experiment with 12 scenarios yielded 48 valid samples, and a hierarchical paired permutation test evaluated design effects. The prototype design increased composite VPF index by 1.9 (4.6%) relative to ordinary design, with significant improvements in structural feature parameters ($p < 0.05$), supporting the assessment capability of the model. Prototype designs consistently enhanced key semantic information (visual guidance facilities and roadway) and reduced cognitive resistance by 2.2% and showed favorable medium-term and long-term stability. Simultaneously, engineering optimization should prioritize entrance areas and the saliency design of visual guidance facilities and traffic signs.

1. Introduction

1.1. Background

Recent years, China's transport network is expanding westward into deeply incised gorges and plateau margins, and transport corridors in complex-terrain regions are increasing markedly. Under constraints of constructible space and cost, spiral tunnels are increasingly being planned and implemented as key nodes of mountainous transport corridors because they enable elevation gain within limited footprints. A spiral tunnel typically consists of a series of continuously aligned curves; while this geometry helps overcome topographic barriers, it also induces pronounced driving cognition challenges (Du et al., 2023). With long, continuous curvature and the superposition of multi-source visual guidance information, drivers must repeatedly judge alignment, adjust speed, and re-evaluate risk within short time windows, leading to cognitive demands that differ substantially from those in ordinary tunnels (Xing et al., 2025a). Naturalistic driving experiments show that spiral-tunnel geometric configurations significantly affect drivers' physiological workload and stress perception as reflected by HRV and related measures (Han et al., 2025a). Complementary work reports pronounced differences in visual attention and subjective workload between spiral and conventional curved tunnels, suggesting that the continuous curvature and constrained sight distance reshape drivers' information-sampling strategies and increase cognitive load (Han et al., 2025b). Furthermore, pronounced portal-related control perturbations near spiral-tunnel entrances and exits have been reported (Xing et al., 2025b).

The constrained visual environment inherent to curved tunnels means that any hazardous event can result in severe consequences (Zhang et al., 2022). Although spiral-tunnel sections are commonly equipped with delineators, alignment guidance devices, lighting, and traffic signs (Ren et al., 2025), practice often shows inconsistent configuration forms and parameter choices, as well as non-standard

* Corresponding author.
E-mail address: zhangchi@chd.edu.cn (C. Zhang).

https://doi.org/10.1016/j.aap.2026.108574
Received 9 January 2026; Received in revised form 17 April 2026; Accepted 27 April 2026

combinations. In addition, spiral tunnels generally entail high construction costs: larger radius tend to offer greater safety but incur higher cost, whereas smaller radii carry higher risk yet remain attractive under budget constraints. Therefore, to reconcile the cost–safety trade-off, spiral-tunnel driving environments should be optimized based on quantifiable cognitive and safety performance. Therefore, a system-level design approach for spiral-tunnel driving environments is proposed from the perspective of driver cognition, and an evaluation model is developed to quantitatively assess its effectiveness, with the aim of reducing drivers' cognitive load and achieving an improved safety–cost balance.

1.2. Literature review

Self-explaining road (SER) theory provides a promising pathway to address cognitive challenges in spiral tunnels by promoting consistency between drivers' expectations and the road environment, thereby enabling drivers to read the roadway and respond appropriately. In recent years, an increasing body of research has introduced SER theory into tunnel contexts. Jiao et al. (2022) have investigated the self-explaining performance of visual guidance facilities in urban underwater tunnels and have reported that vertically spaced installations deliver superior self-explaining effects. Yan et al. (2024) have further incorporated drivers' visual behavior and have shown that colored pavement and light-toned inner-wall decoration can enhance a tunnel's self-explaining performance. Xing et al. (2025a) have examined the self-explaining effects of different visual guidance facilities in spiral tunnels based on drivers' spatial perception and allocation of visual attention, and have found that edge markings are the most effective. Overall, extensive studies have explored optimization of tunnel driving environments, achieving substantial progress in evaluating local elements such as visual guidance facilities, safety signage, and pavement color (Jiao et al., 2022; Xing et al., 2025a; Yan et al., 2024). These efforts provide robust empirical evidence supporting the safety relevance of SER theory at the facility level.

However, as SER theory has been applied to a wider range of contexts, facility-level studies have increasingly revealed the need to transition toward system-oriented design. Accordingly, a critical question has remained: How should a self-explaining tunnel roadway be designed? This question concerns not only incremental improvements to individual devices, but also the holistic perception that drivers form while navigating space. Van der Horst and Kaptein (1998) have found that when road designs are consistent within each category and clearly distinguishable across categories, drivers can classify roads more accurately and exhibit more balanced and consistent driving behavior. Theeuwes (2021) has argued that drivers develop road-type schemas and expectations through long-term experience, and that only roads with clear categorization, distinctive appearance, and standardized design can reliably trigger consistent behavior. Dutch guidelines have explicitly required that each road be classified prior to construction or reconstruction, with each category adopting a unique and standardized appearance and facility configuration (Boender, 2014). This approach essentially triggers drivers' expectations for specific road types immediately through standardized road environment, thereby naturally guiding expected driving behavior, which is named road prototype design in this study. Compared to optimizing isolated facilities one by one, road prototype design can determine the target driving expectations based on the operational needs of the road, and then organize multiple environmental elements in a coordinated manner to support these expectations, thereby creating an integrated environment consistent with the expected driving conditions.

Due to the subjectivity in the definition of SER, previous studies on the evaluation of SER-based interventions have adopted various methods depending on their approach, including questionnaires (Theeuwes et al., 2024), perception experiments (Xia et al., 2025), and driving simulation studies (Xing et al., 2025a). For example, Jiao et al. (2022) have conducted speed-perception experiments to systematically assess the self-explaining performance of various visual guidance facilities in urban tunnels, yet this approach has struggled to capture the geometric specificity of spiral tunnels. Some studies have attempted to improve drivers' cognitive states by optimizing spiral-tunnel walls or visual guidance facilities. In particular, Yan et al. (2024) and Xing et al. (2025a) have used driving-simulator experiments and have evaluated self-explaining performance through behavioral and eye-tracking measures, such as spatial perception and lane deviation; however, these efforts still have some limitations when applied to spiral tunnels. Although numerous scientific methods have been employed, considering the large curve angles in spiral tunnels (where drivers must travel along a curve with the same direction and radius for a long period), it is necessary to capture continuous cognitive indicators to assess the dynamic characteristics of driver cognition. Furthermore, due to technical limitations, while previous studies have validated the effectiveness of environmental interventions, few have examined the parameterization of environmental information, making it difficult to directly correlate changes in cognitive indicators with environmental changes. Therefore, it is equally crucial to establish a cognitive evaluation method based on the parameterization of the environment to validate the effectiveness of environmental interventions.

Driving cognition is jointly regulated by the spatial layout of information channels and their activation levels within the visual workspace (Chen et al., 2025). This regulation is constrained by the interaction between the dynamic salience of environmental elements and drivers' prior experience, which in turn forms a coupled mechanism linking attention allocation and response speed (Li et al., 2023; Steelman et al., 2017). Therefore, relying solely on behavioral performance or isolated physiological indicators may not fully reveal the mechanisms through which self-explaining performance emerges. Environmental elements, as cues that convey critical information or trigger perceptual responses (Lindenberg, 2018), require explicit consideration of how they are perceived, interpreted, and translated into driving actions in dynamic driving processes. However, studies have tended to treat attention allocation as a quasi-static construct and have adopted simplified gaze-tracking or static AOI techniques, without deeply integrating dynamic contextual factors (Kanaan et al., 2024).

In this context, environmental semantic segmentation provides a new perspective for dynamically identifying and analyzing the mechanisms through which different environmental elements contribute to self-explaining roads. In the United States, research on Self-Enforcing Roads has been actively exploring assessment systems based on image recognition and data modeling, emphasizing the use of road-environment design to encourage drivers to self-enforce target speeds and thereby reduce the risk of severe crashes (Talebpour et al., 2024). Ren et al. (2024) have developed a visual road semantic-segmentation model coupled with a visual-sensitivity model, enabling semantic identification and quantitative analysis of environmental elements on rural roads and laying a foundation for mechanistic quantification of environmental effects. In tunnel contexts, a growing body of work has examined how environmental elements influence driving cognition. Han et al. (2025c) have investigated the effects of roadway geometry on drivers' visual presence. Zeng et al. (2023) have reported that appropriate sign information content and layout can improve sign visibility and drivers' response speed. Bei et al. (2024) have shown that visual guidance facilities placed at different locations can provide more decision time and support clearer path judgment in curves. Zheng et al. (2025) have found that rhythm visual guidance design can significantly enhance drivers' perception of tunnel sidewalls and lateral trajectories, reduce driving fatigue. In addition, He et al. (2017) have reported that higher wall luminance improves the inner visual environment, mitigates visual fatigue, and enhances driving safety. Overall, existing research on the impact of different facilities on driver cognition strongly supports our classification of environmental facilities: these facilities will be categorized and optimized according to road prototype design

principles, while the contribution of each facility category to visual perception will be validated in the model.

1.3. Aim of study

Overall, despite significant progress in research on tunnel self-explanation optimization, the following issues remain when addressing spiral tunnel scenarios and system-level environmental intervention facility design: (1) Current studies mainly focus on the improvement of driver cognition by a specific category of tunnel facilities, lacking a system-level environmental design approach. This may cause the benefits of environmental intervention facilities to depend on the context, limiting their scalability and practical value; (2) Current research uses environmental intervention facilities to improve driver cognition, but due to technical constraints, there is limited parameterization of environmental information, making it difficult to directly relate changes in specific environmental information to cognitive improvement at the data level, thus limiting the interpretability of results; (3) Given the unique characteristics of large curve angles in spiral tunnels, existing evaluation methods struggle to dynamically quantify cognitive states during the driving process, potentially overlooking the distinctive cognitive features.

Therefore, it is essential to propose a system-level tunnel environment facility design method, allowing for its potential application in tunnel projects of varying scales while balancing safety and cost. At the same time, it is necessary to parameterize environmental information in the evaluation process to clarify the contribution of specific environmental factors to cognitive improvement, and to dynamically study the cognitive characteristics of drivers in spiral tunnels. Thus, we have undertaken the following work: (1) proposed a system-level tunnel environment facility design method—the road prototype design method; (2) parameterized environmental information through semantic segmentation and established a dynamic evaluation model based on the visual-perception fluid; (3) validated the feasibility of the proposed method and model; and (4) analyzed the mechanism of cognitive improvement due to changes in driving cognition and environmental facilities in spiral tunnels.

2. Methods

2.1. Road prototypes design based on environment-perception consistency

2.1.1. Design method

As discussed in Section 1, when driving on roads with similar appearances, drivers tend to subjectively classify them as the same prototype and adopt consistent driving behaviors to complete the driving task. This categorization relies more on drivers' experience and holistic environmental cues than on the formal technical class of the road. By aligning environmental cues with the intended road function, designers can prompt drivers to adjust their behavior and thereby reduce risk (Theeuwes et al., 2024). In this study, the road prototype is not only a set of roads with similar visual appearance, but also corresponds to specific driving expectations as an environmental design unit at the system level. Therefore, prototype design refers to a coordinated design process where road geometry, target operating conditions, expected driver mentality, and multiple environmental elements are jointly considered to ensure that the overall environmental cues consistently support the expected driving behavior. This differs from traditional design methods, which primarily focus on optimizing individual facilities or adjusting local parameters separately. The design workflow is summarized in Fig. 1.

2.1.2. Road prototypes design for spiral tunnels

For spiral tunnels, the radius has been shown to significantly influence cognitive load (Han et al., 2025c), driving behavior (Xing et al., 2025a), and vehicle control near tunnel entrances and exits (Xing et al., 2025c). Thus, in the present spiral-tunnel context, radius category is used as a basis for distinguishing prototype types, as different radii are associated with different operating demands and driving expectations. Meanwhile, for research purpose, a threshold of 600 m was adopted to distinguish between small and large radii based on relevant studies.

Table 1
Stepwise road prototype design for large- and small-radius spiral tunnels.

Step	Large-radius spiral tunnel	Small-radius spiral tunnel
Step 1: Define road characteristics	Larger curve radius with a long same-direction curvature.	Smaller curve radius with a long same-direction curvature.
Step 2: Define environmental design objectives	Guide drivers to maintain a relatively high cruising speed while avoiding lane changes and ensuring stability of both speed and lane position.	Guide drivers to proceed cautiously at a lower speed, avoid lane changes, and maintain stability of speed and lane position.
Step 3: Specify target driving mindset and behavior	Maintain alertness and stability under high-speed conditions. Sustain a relatively high speed under safe conditions and remain stable within the lane.	Reinforce cautious expectations under low-speed conditions. Avoid lane changes, traverse the tunnel at a relatively low speed, and maintain stable speed and lane position.

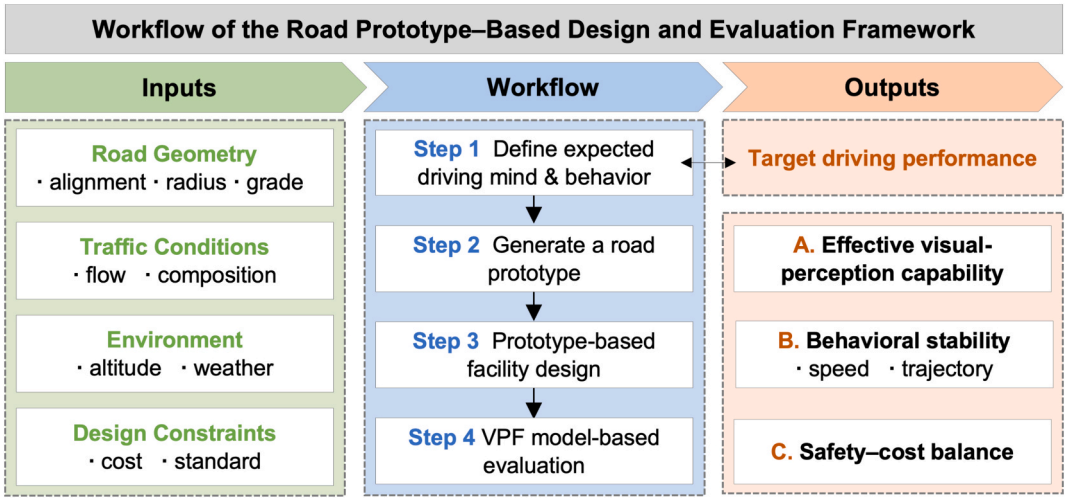

Fig. 1. Flow chart of road prototype-based design.

Their design steps are presented in Table 1.

Building on drivers' visual search and attention-allocation characteristics and the open-road semantic taxonomy proposed by Ren et al. (2024), we categorized tunnel-environment semantics into four groups: (i) visual guidance facilities (lamps, retroreflective rings and land marks); (ii) traffic signs (traffic signals and speed-limit signs); (iii) the overall environment (sidewalls, linings, and maintenance walkways); and (iv) the roadway (road surface and lines). Qualitative configurations of the four facility categories under different prototype conditions are summarized in Table 2. Detailed quantitative parameters and design renderings are specified in Section 3.2.

2.2. Visual-perception fluid model

The Visual-Perception Fluid (VPF) model is a quantitative analytical framework inspired by fluid mechanics and information-dynamic representations, and organized through a fluid-based descriptive language. The purpose of introducing this framework is to provide a more intuitive and quantifiable way to describe how visual information is acquired and associated with cognitive burden in complex roadway environments. Information theory has been widely used to characterize cognitive processes such as encoding, control, and prediction (Sayood, 2018). In the brain, information processing involves top–down cognitive control and can be meaningfully described in terms of the flow, rate, and stability of information dynamics (Rabinovich et al., 2012). From a physical standpoint, visual sensing is enabled by light, which propagates at an extremely high speed ($\approx 3 \times 10^{10}$cm/s) and is mapped onto the retina almost instantaneously. When information is treated as moving carriers with effective mass, their dynamics can be described using fluid-mechanics primitives, where key state variables include density, velocity, resistance, and kinetic energy (Iida et al., 2012). Meanwhile, visual attention is commonly conceptualized as a finite and allocable resource closely linked to task demands and behavioral performance (Theeuwes, 2025). Mental workload (MWL) is typically interpreted as an intermediate outcome of partially separable information-processing demands; as task demand increases, resource competition intensifies and is regarded as a form of cognitive-resource loss, which in driving may manifest as slowed responses and degraded performance (Faidah et al., 2026).

Building on the above foundations, we model the external roadway scene as a "particle field" of visual information units and represent drivers' visual perception as an information flow (Fig. 2). Drivers' sampling of environmental information arises from the interaction between (i) goal-directed intention and (ii) the physical properties of the visual environment. The information-sampling rate depends on both the refresh rate and the coverage of sampled information, which can be operationalized by scanning amplitude and scan count (Alyan et al., 2026). The loss of visual-attention resources is represented by driving workload. However, prior evidence suggests that an excessively high sampling rate (e.g., enlarged saccade amplitude) may itself exacerbate driving workload and thereby increase the loss of visual-attention resources. To quantify this, we introduce the concept of effective visual-perception capability (Kujala et al., 2023). This capability is operationalized by combining the information-sampling rate and cognitive workload, providing an abstract measure of the effective margin between perceptual input and cognitive load. Finally, integrating the driving decision-making model (DDM) and cognitive-flow perspectives, we assume that driving actions occur when the visual capacity relevant to a candidate DDM option reaches a threshold (Rabinovich et al., 2012; Wang et al., 2020; Yang, 2025).

2.2.1. Equivalent mass of information

We used environmental semantic segmentation to quantify the information composition of facility environments (Ren et al., 2024). Because Mask2Former aligns more closely with human visual-attention patterns in image parsing (Cheng et al., 2021), its high-accuracy pretrained model was adopted to decompose each road-scene image into semantic labels and mask arrays, as shown in Fig. 3. The model then output each semantic label, together with the class-wise counts n_j and size information p_{ij}.

After semantic segmentation, we used the pixel share of each semantic patch (Ye et al., 2025) to represent the objective density of environmental information flow at time i, denoted as ρ_{ij} (Li et al., 2023), as defined in Eq. (1). The information provided by the environment is converted by ρ_{ij} into an objective, extractable measure of semantic quantities, enabling a comparable quantification of information contributions across different types.

$$\rho_{ij} = p_{(i+1)j} \times n_{(i+1)j} \tag{1}$$

where, i denotes the time unit. Consistent with drivers' preview characteristics (Wolfe et al., 2022), the parameters of the current unit (i) is derived from the environmental image at the next unit $(i+1)$ location; The index j denotes the semantic category $(j = 1-4)$, corresponding to the four semantic groups defined in Section 2.1. The term $p_{ij}(\mathrm{px})$ denotes the pixel size of an individual semantic mask within category j, and n_j denotes the number of segmented instances in category j.

Account for the stochasticity and fuzziness of human information processing, we compute information weights using a Shannon-entropy variant (Li et al., 2023). Specifically, the input information-quality vector is defined as $u_j \in [0,1], j = 1,2,3,4$. For each membership value

Table 2
Facility design scheme for prototype-designed spiral tunnels.

Categories of tunnel facilities	Facility	Relationship with driving performance	Reference	Ordinary design	Prototype design (large-radius)	Prototype design (small-radius)
Visual Guidance Facilities	Density of retroreflective rings	Positively correlated with speed stability.	Wang et al. (2025b)	Low	Low	High
	Edge markings	May cause drivers to reduce their speed consciously.	Jiao et al (2023)	None	None	Present
	Density of chevron alignment signs	Positively correlated with lower speed.	Rose and Carlson (2005)	Medium	Low	High
Traffic Signs	Density of traffic signals and speed limit signs	Positively correlated with lower speed and higher visual load	Zeng et al (2023)	Medium	Medium	High
Overall Environment	Lighting color temperature	Positively correlated with higher driving load, better speed and lane-keeping ability.	Song et al (2024)	Medium	Low	High
	Color of sidewalls	Positively correlated with speed and lane-keeping stability	Kircher and Ahlstrom (2012)	Longitudinal blue bars (neutral tone)	Light gray (neutral tone)	Light yellow (warm tone)
Roadway	Color of lane separation lines	Yellow lines lead to better speed and lane-keeping stability	Parham et al (2003)	White	White	Yellow

Note: The ordinary design refers to the environmental facility design of a typical spiral tunnel in western mountainous regions of China. Compared with the ordinary design, the prototype designs differ only in the items listed above; other aspects such as lighting type, lane width, and tunnel cross-sectional shape remain identical.

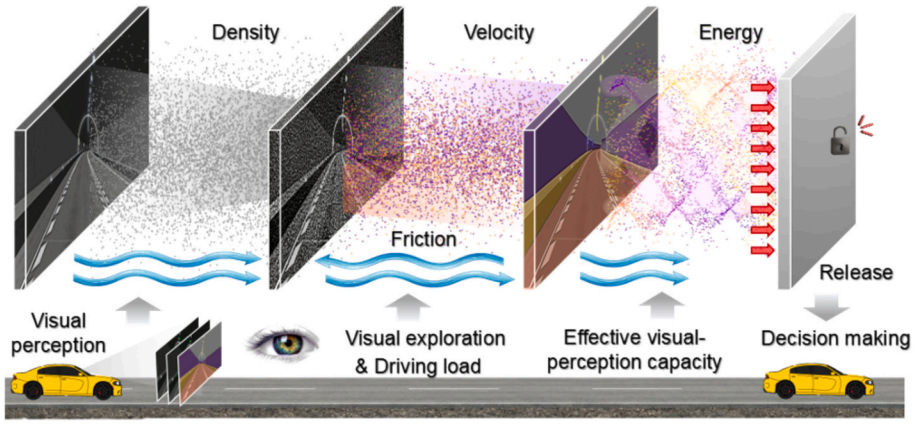

Fig. 2. Analogy diagram of VPF model.

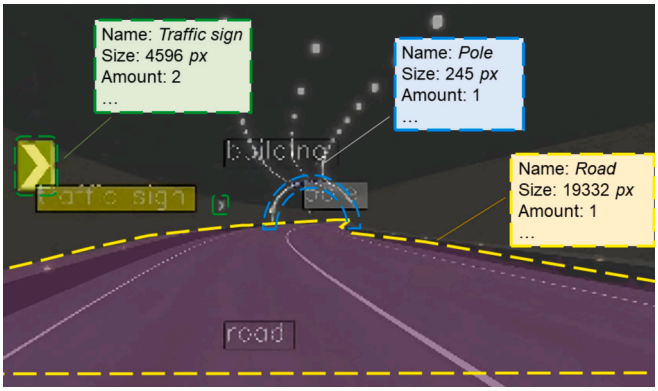

Fig. 3. Diagram of environmental semantic segmentation.

u_j, the exponential term g_j of the binary fuzzy entropy is calculated (Eq. (2)). Drivers' subjective importance allocation across semantic categories is incorporated by g_j, thereby accounting for how perceived importance shapes the distribution of visual-attention resources within the model.

$$g_j = \frac{exp[-u_j \cdot \ln(u_j) - (1-u_j)\cdot \ln(1-u_j)]}{\sum exp[-u_j \cdot \ln(u_j) - (1-u_j)\cdot \ln(1-u_j)]} \tag{2}$$

Accordingly, the environmental information quality M_i is defined as a combination of the information salience assigned by the driver and the inherent significance of the environmental semantics (Eq. (3)), according to subjective expected utility (Li et al., 2023). This indicator is highly sensitive to changes in environmental semantics and can directly differentiate the scenario-specific environmental parameters. It should be noted that this indicator is only a functional analogy for characterizing environmental information and does not imply that information has a physical mass in the literal sense.

$$M_i = \rho_{ij} \times g_j \tag{3}$$

2.2.2. Velocity of information flow

Based on visual-attention resource theories (Li et al., 2023; Wickens, 2015), saccade amplitude is used as an indicator of drivers' visual information sampling, reflecting the spatial extent of attentional switching across multiple areas of interest. Consistent with prior driving evidence, demanding events may elicit larger and more frequent saccades, suggesting broadened sampling that can be beneficial for coverage but may also be accompanied by increased workload (Alyan et al., 2026). Let the saccade amplitude (px/s) for environmental information acquisition be represented by a distance measure. The velocity at which a driver receives visual information per unit time Δt is defined by Eq. (4).

$$V_i = \frac{l_{ampli}}{\Delta t} \tag{4}$$

2.2.3. Cognitive resistance

Fixation duration reflects the time that gaze remains on a specific point or region, and longer fixations are commonly regarded as an objective proxy for higher processing difficulty or greater subjective importance (Liu et al., 2022; Souza and Freitas, 2022). The LF/HF ratio is a frequency-domain HRV index and is widely used to quantify stress level and mental workload; a higher LF/HF ratio generally suggests sympathetic dominance and a higher cognitive load (Raza et al., 2024). According to attention resource theory and the energy-efficiency perspective of decision-making (Greaves, 2013), cognitive resource consumption can be modeled as the product of information subjective importance and cognitive load (Li et al., 2023), implying that cognitive resistance increases when environmental information is more important and neural activation is higher. Because human information processing is inherently stochastic, we used a windowed single-scale sample entropy (SampEn) to capture the influence of irregularity in physiological signals ($m = 2$, $r = 0.2\sigma$, $\ell\infty$distance, no self-matches) (Raza et al., 2024). Accordingly, cognitive resistance at time i, denoted as F_i, was approximated by Eq. (5):

$$F_i = SampEn(r_i \times T_i) \tag{5}$$

where r_i represents the normalized LF/HF ratio and T_i(ms) represents the normalized fixation duration.

2.2.4. Composite VPF index

Finally, the composite VPF index P_{ci} was proposed, as a tool for measuring current visual-perception capability under environmental information-flow stimulation. This index combines the equivalent mass of information, velocity of information flow, and cognitive resistance, inspired by the principles of Darcy–Weisbach formulation (Eq. (6)). However, it should be emphasized that the P_{ci} serves as an abstract measure designed to characterize the relationship between attention resource and cognitive workload, rather than energy-related concepts.

$$P_{ci} = \frac{1}{2}M_i V_i^2 - F_i V_i \Delta t \tag{6}$$

To validate the ability of P_{ci} to distinguish between different visual-perception capacity across various driving conditions, concurrent criterion-related validation will be used. This will compare P_{ci} with established safety criteria such as acceleration and trajectory deviation to assess its predictive effectiveness in real-world driving behavior.

2.2.5. Path analysis

Path analysis quantifies both the direct effects of explanatory variables on dependent variables and their indirect effects through mediating variables, and it aims to provide a supplementary interpretive framework for identifying possible effect directions and relative contributions. In this study, the V_i and F_i were used as mediators, and the V_i was assumed to exert a certain mediating effect on the F_i. The composite VPF index P_{ci} was specified as the outcome variable to capture the relative contributions and effect directions of the four environmental semantic indicators on cognitive performance, as shown in Fig. 4. Considering that the relationship between the P_{ci} and behavioral outcomes will be validated through concurrent criterion validity analysis, behavioral indicators were not included in the path analysis. The detailed path model is provided in the Appendix A.

3. Experiment design

3.1. Experimental platform and equipment

A multi-degree-of-freedom custom-built driving simulator with high fidelity was used. The platform architecture and data acquisition devices are shown in Fig. 5, including a complete instrument panel, steering wheel, accelerator module, gear-shift module, and user-interface buttons. The display system consisted of three independent 2 K-resolution screens, providing a vertical field of view of 28° and a horizontal field of view of 150°. In addition, a low-intrusion eye tracker (7invensun aSee Glasses) and a wristband (PsychTech multimodal wristband and computational kit) were used to monitor participants' visual and physiological data, respectively.

Fig. 5. Experimental platform and equipment.

3.2. Experimental scenarios

The experimental scenarios were jointly developed using the UC-win/Road V8.1 driving simulation platform and SketchUp 2024. A full circular horizontal curve with a 155° central angle was adopted, and a constant longitudinal grade of 2.8% was applied throughout the tunnel segment (uphill for left-turn scenarios), together with lane layout, arch-shaped, and lighting type to represent a spiral tunnel in mountainous western China. The ordinary scenario was used as the baseline and was set up to match this real tunnel configuration as closely as possible, including the full set of facility installations (Fig. 6).

Facility parameters and schematic representations of the simulated tunnel are shown in Table 3. All facility designs were developed in accordance with the Chinese specifications for tunnel traffic safety facilities. The unit definition and spacing calculation method for retroreflective rings followed Du et al. (2021). The corresponding spacing values for different numbers of visible rings under varying conditions are provided in Appendix B Table B2.

The 12 scenarios follow a controlled grouping design. The selected radii represent both typical built spiral-tunnel scales (500 m as the smallest and 970 m as the largest) and a forward-looking lower-bound condition (250 m). Specifically, R = 250 m was included as the minimum curve radius allowed for expressways in (Specifications for Highway Geometric Design, 2017), to evaluate perception and facility-design performance under highly constrained terrain. Three spiral radii (R = 970 m, 500 m, and 250 m) and two turning directions (left and right) form six geometry-fixed groups. Within each group, the spiral alignment and simulation settings were kept identical, and only the facility design scheme was changed (ordinary and prototype), yielding 12 scenarios in total (Fig. 7). To avoid confounding effects due to potential left–right geometric asymmetry, left- and right-turn cases were modeled separately but with the same nominal radius and identical lane conditions. The large-radius prototype design was applied to R = 970 m, whereas the small-radius prototype design was applied to R = 500 m and 250 m.

3.3. Participants

To ensure the representativeness and generalizability of the experimental data, the sample size was determined using Eq. (7) based on the expected variance, the target confidence level, and the allowable margin of error.

$$n = \frac{Z^2_{\alpha/2}\sigma^2}{E^2} \tag{7}$$

where n is the sample size, $Z^2_{\alpha/2}$ is the standard normal distribution statistics, σ is the standard deviation, and E is the maximum error.

In this study, a 95% confidence interval was selected, σ was 0.25, and E was 10%. The minimum calculated sample size was determined to be 23. Finally, 53 participants were recruited, with a gender distribution reflecting that of Chinese drivers (Xinhua News Agency, 2022). All participants held valid driving licenses, had adequate driving experience, and had normal or corrected-to-normal vision. In this study, 5 participants reported discomfort; therefore, 48 valid datasets were obtained. The male participants were aged 20–47 years (M = 32.32, SD = 6.80), and the female participants were aged 21–48 years (M = 29.97,

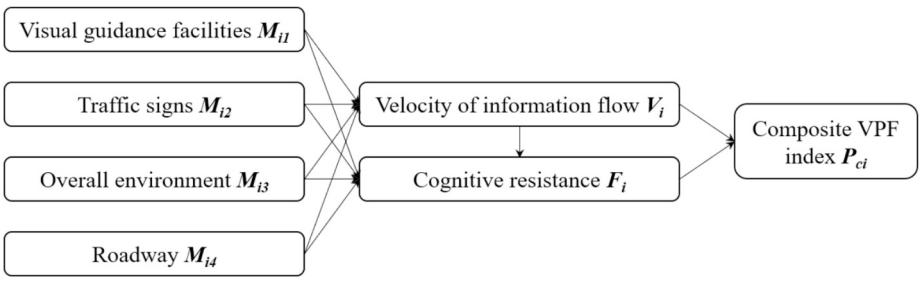

Fig. 4. Diagram of path analysis.

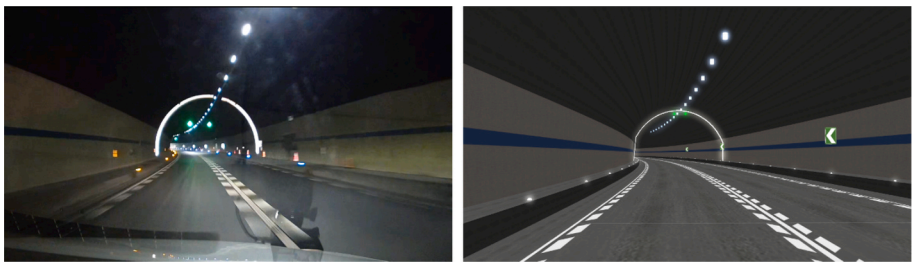

Fig. 6. A visual comparison between the real-world scene and the corresponding simulated scene.

Table 3
Facility parameters for ordinary and prototype-designed spiral tunnels.

Facility	Ordinary design	Large-radius prototype	Small-radius prototype
Retroreflective rings			
Edge markings	1 visible 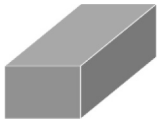	1 visible 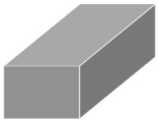	3 visible 
Chevron alignment signs	None 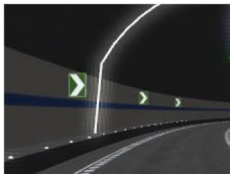	None 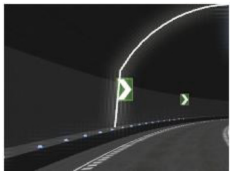	Present 
Traffic signals	30 m spacing	50 m spacing	20 m spacing
Speed limit signs	200 m spacing	300 m spacing	100 m spacing
Lighting	200 m spacing 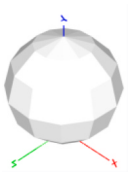	300 m spacing 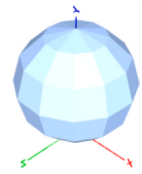	100 m spacing 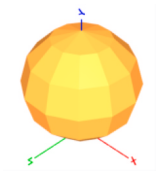
Sidewall	RGB (255, 255, 255) 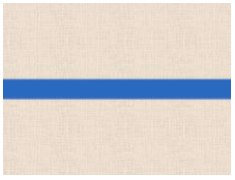	RGB (159, 191, 239) 	RGB (255, 184, 113) 
Lane separation lines	Longitudinal blue bars 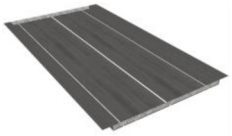	Light gray 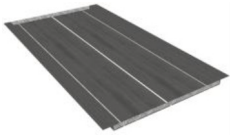	Light yellow 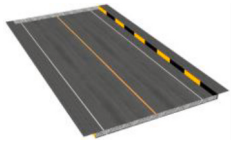
	White	White	Yellow

SD = 6.34). Other information is presented in Table 4. No participant was informed of the study purpose. Participants received compensation, and they were informed that all collected data would remain anonymous and be reported only in an aggregated manner.

To ascertain the adequacy of the participant count for detecting meaningful differences of P_{ci} between the ordinary and prototype con-

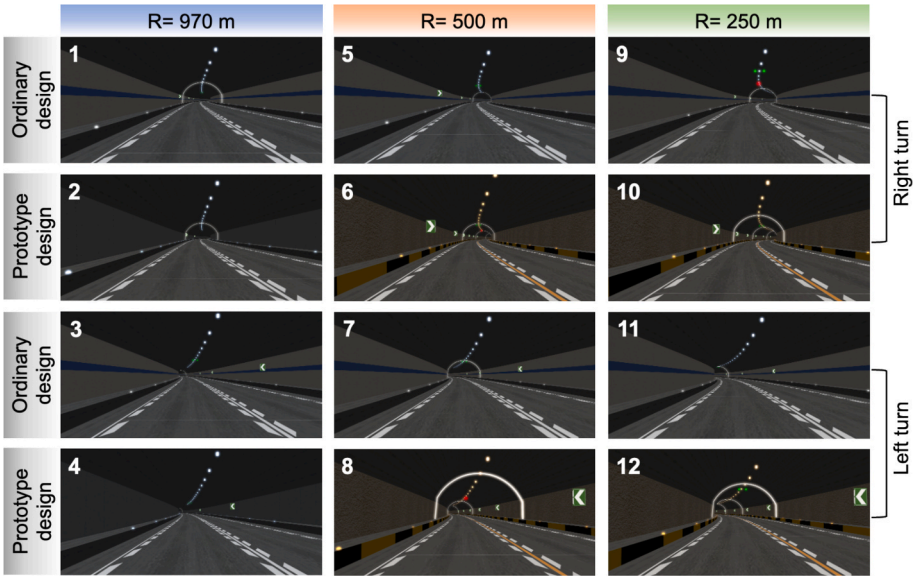

Fig. 7. Rendering of all driving simulation scenes.

Table 4
Basic information of participants.

Variable	Gender		Tunnel driving experience		Driving age (year)		Actual driving mileage (km/year)	
Description	Females	Males	Yes	No	4 or below	5 or more	≤10,000	>10,000
Frequency	17	31	27	21	24	24	31	17

ditions, an a priori power analysis was performed in MATLAB using a two-sample *t*-test. The results indicate that, at $\sigma = 0.10$ confidence level, the achieved statistical power is 0.890, exceeding the commonly accepted threshold of 0.80. Additionally, the Cohen's d for the comparison between conditions was found to be 1.16 (95% CI: 0.73–1.59). These results indicate that the study is adequately powered to detect the effects under investigation.

3.4. Experimental procedure

The experiment consisted of a practice session and a formal session: (i) During practice, detailed instructions on the driving simulator were provided, and four driving trials were completed to familiarize participants with the virtual environment. (ii) Before the formal session, the eye tracker and wristband were fitted with assistance from the staff, and participants were briefed to ensure that the instrumentation had negligible influence on driving behavior. (iii) During each scenario, participants were only instructed that the in-tunnel speed limit was 80 km/h and that passenger cars should keep to the left; they were asked to drive freely according to their habitual driving style and real-time responses to the simulated environment. (iv) After each scenario, drivers were provided with sufficient rest. Scenario order was randomized and counterbalanced by Latin-square method across participants to mitigate learning habituation and sequence effects. Participants completed all scenarios individually, and the procedure was repeated until all participants finished the experiment in a quiet, isolated, and dedicated room to avoid external distractions.

3.5. Data measurement and alignment

For each scenario, variables listed in Table 5 were recorded, and participant-level averages were used to reduce the influence of individual differences. To enable continuous characterization of multi-source data across conditions and avoid discretization errors

Table 5
Experimental measurement variables.

Variables	Frequency	Index	Description
Semantic size and count	/	$p_{(i+1)j}$, $n_{(i+1)j}$	Captured from images taken from the simulated road.
Significance of semantics	/	u_j	Derived from participants' semantic rating scores.
Fixation duration	1000 Hz	T_i	Directly exported from the software.
Saccade amplitude	1000 Hz	V_i	Directly exported from the software.
LH/HF ratio	100 Hz	r_i	Computed and exported by the software.
Acceleration ($m{\cdot}s^{-2}$)	10 Hz	a_i	Directly exported from the software.
Trajectory deviation (m)	10 Hz	d_i	Directly exported from the software.

associated with single-threshold criteria (Wang et al., 2024), the time series were aligned using windows based on the cumulative turning angle of the spiral tunnel. The angle was segmented into equal windows, and each window was treated as a time unit, indexed by *i*, which was used as a standardized reference axis (Fig. 8). Within each window, the mean of observations over the angle range was computed to represent the variable value.

4. Results

4.1. Validation

4.1.1. Statistical analysis

First, to determine whether the road prototype design method proposed in Section 2.1 produced an empirical improvement in driving cognition and safety, the prototype-design outcomes were compared

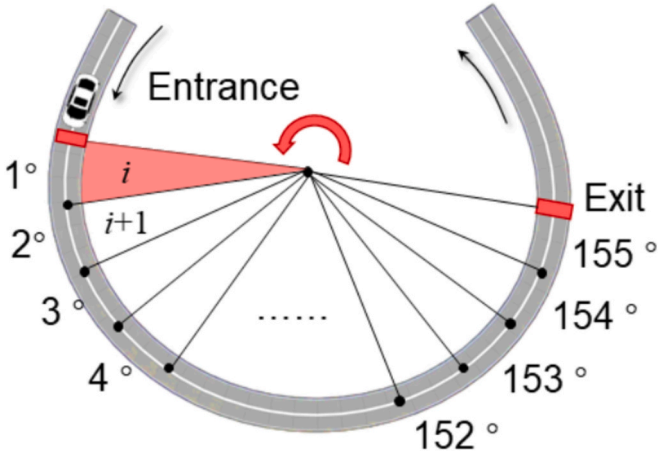

Fig. 8. Schematic diagram of windows division by spiral angle.

with those of the ordinary design under large-radius and small-radius scales. As summarized in Table 6, the prototype design increased the P_c by 1.9 (4.6%) overall. The improvement was 1.1 (3.3%) under the large-radius condition and 2.4 (6.2%) under the small-radius condition. These results indicate that the proposed road prototype design yielded a measurable enhancement in drivers' visual-perception capability relative to the ordinary design.

4.1.2. Construct validity test

To verify whether the VPF model described in Section 2.2 could systematically detect the cognitive improvement induced by prototype-based environment design, a construct validity test was conducted. Specifically, within each stratum defined by radius and turning direction, the prototype design was paired with the ordinary design, yielding six paired comparisons. Structural features were extracted from P_c, including the mean (P_{c_mean}), the 95th percentile (P_{c_p95}), the maximum (P_{c_max}), and the peak count (P_{c_nPeaks}), to test whether the prototype design shifted P_c upward overall.

As the sample consisted of six paired differences and did not satisfy the assumptions of classical parametric tests, a stratified paired permutation test was adopted. Under the null hypothesis that the prototype design did not change P_c, the signs of the paired differences were flipped to construct the exact null distribution of the observed mean difference (*obsMean*), from which two-sided and one-sided (prototype > ordinary) p values were obtained. As reported in Table 7, the prototype design produced consistent positive increases in P_{c_mean}, P_{c_p95}, and P_{c_max} (one side), and the effects were statistically significant ($p < 0.05$), indicating that the prototype design significantly increased P_c after controlling for radius and turning direction, thereby supporting the construct validity of the model. By contrast, the mean paired difference in peak count was (−1.5) and was not significant ($p > 0.05$), suggesting that peak counts are more susceptible to fluctuations.

4.2. Results of road prototype design

4.2.1. Equivalent mass of information

Comparisons of information-mass outcomes across the six conditions are shown in Figs. 9 and 10. Compared with ordinary design, the prototype design significantly increased the equivalent information mass of both the roadway and visual guidance facilities across almost all conditions. Turning direction exhibited no clear influence on information mass, indicating that this factor did not drive either the geometric–semantic composition or the subjective weighting of information. Specifically, M_{i1} (visual guidance facilities) and M_{i4} (roadway) under the prototype design were higher than those under the ordinary design in all conditions. Under the large-radius condition, the prototype design slightly increased M_{i2} (traffic signs) relative to the ordinary design, whereas M_{i3} (overall environment) was consistently lower under the prototype design than under the ordinary design. Another point is the equivalent mass of environmental elements is jointly influenced by curve radius and turn direction. Although the roadway layout was kept consistent across these scenarios, differences in visual occlusion and viewing angle may lead to substantial differences between left- and right-turn conditions.

Table 6
Calculation results of indicators with different road design methods.

Scenarios		M_i	V_i	F_i	a_i	d_i	P_c
Large-radius	Ordinary	0.25	0.91	0.85	0.87	1.01	43.0
	Prototype	0.31	1.05	0.75	0.87	1.02	44.4
Small-radius	Ordinary	0.26	0.60	0.72	1.02	1.06	38.8
	Prototype	0.31	0.64	0.79	1.18	1.10	41.2

Table 7
Results of the construct validity assessment.

Index	*obsMean*	$p_{(\text{two side})}$	$p_{(\text{one side})}$	Results
P_{c_mean}	1.97	0.0625	0.03125	Significant (one side)
P_{c_p95}	2.78	0.0625	0.03125	Significant (one side)
P_{c_max}	4.39	0.0625	0.03125	Significant (one side)
P_{c_nPeaks}	−1.50	0.625	0.8125	Not significant

4.2.2. Information flow velocity

Results for information-flow velocity, represented by saccade amplitude, are reported in Table 8. Overall, drivers in large-radius conditions exhibited larger saccade amplitudes (right: 1.441 > 1.209; left: 0.653 > 0.594), whereas the small-radius prototype design also slightly increased saccade amplitude (right: 0.628 > 0.622; left: 0.645 > 0.582). Saccade amplitude also varied across locations within the spiral tunnel (Fig. 11). As the cumulative turning angle increased, the large-radius prototype design primarily promoted saccade amplitude in the mid-to-late segments of the tunnel (20°-155°). In contrast, the small-radius prototype design mainly increased saccade amplitude in the mid-section of the tunnel (20°-140°), while the overall fluctuation of the indicator was more gradual.

4.2.3. Cognitive resistance

Results for cognitive resistance, quantified by cognitive load, are summarized in Table 9. Overall, the prototype environment was associated with lower cognitive load, with an average reduction of approximately 0.02 (2.2%). Fig. 12 illustrates the locations where workload differences were most pronounced. Under the ordinary design, higher cognitive load occurred near the exit region in the large-radius scenes (Fig. 12 (a), 80°-150°), and around the mid-section (60°) in the small-radius scenarios. By contrast, the prototype driving environment relatively reduced the overall workload level in the small-radius scenarios.

4.2.4. Results of driving behaviors

Acceleration results are shown in Fig. 13. Under the large-radius scenarios, the prototype curve generally lay below the ordinary curve. Although acceleration increased overall in both designs, the prototype design exhibited a lower peak and smaller fluctuations. For both designs, acceleration increased shortly after the entrance and typically showed a rise–fall pattern before the exit. The shaded area in Fig. 11 marks the pre-exit acceleration-variation zone. The acceleration-variation zone near the exit occurred at 135°-155° for the large-radius condition and 95°-155° for the small-radius condition, indicating a larger and more unstable pre-exit speed-control fluctuation under the small-radius scenarios.

Drivers' lateral deviation in the spiral tunnel is shown in Fig. 14. Overall, the prototype design yielded smaller deviation. Under the large-radius condition, the prototype deviation amplitude was slightly lower

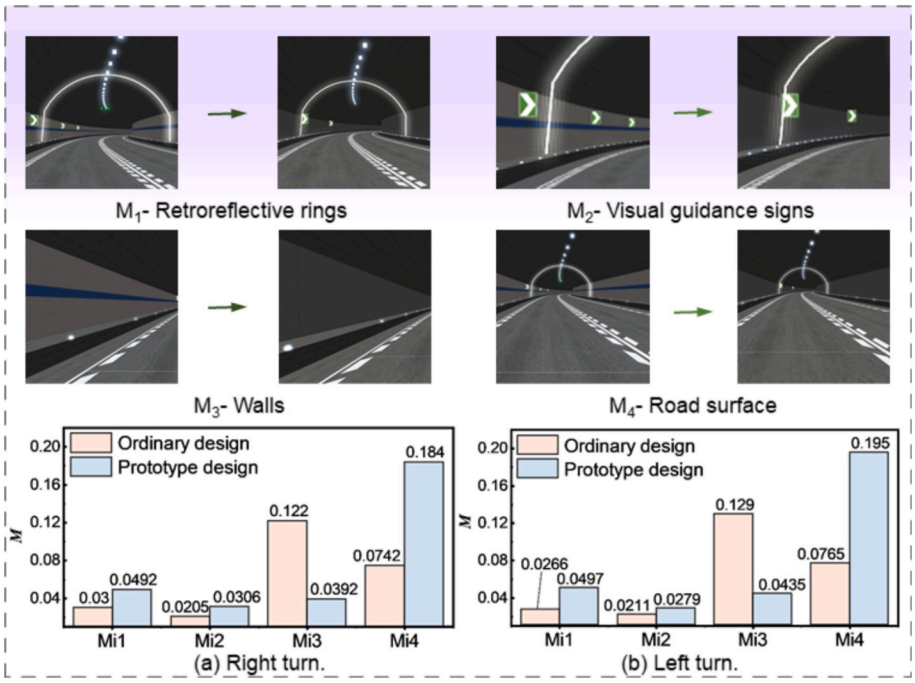

Fig. 9. Equivalent information mass results under large-radius scenarios.

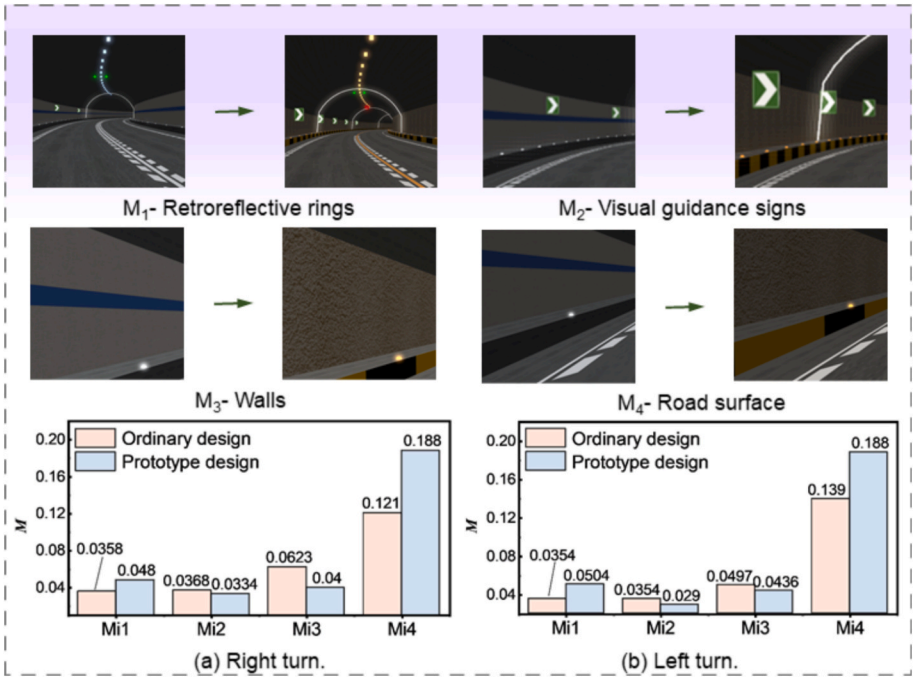

Fig. 10. Equivalent information quality results under small-radius scenes.

than that of the ordinary design throughout the entire internal segment under large-radius condition, with a smoother fluctuation pattern. Under the small-radius condition, the prototype design showed higher overall deviation than the ordinary design, and both designs exhibited significant fluctuation before the exit.

4.2.5. *Composite VPF index*

The computed composite VPF index results P_c are reported in Table 10. Overall, the prototype design yielded higher P_c values than the ordinary design across most of the conditions. The bar charts and the corresponding heat maps in Fig. 15 further showed that observed advantages of the prototype design were primarily concentrated at key locations, including the inner region where stable turning begins (34°), and the tunnel exit (155°). At these locations, the prototype bars were often generally higher than those of the ordinary design, and the color scale shifted toward red, indicating a more pronounced improvement under the prototype design relative to the ordinary design. Results of the criterion-related validity (Spearman correlation) showed that P_{ci} was negatively associated with both acceleration and lateral deviation in 11 out of 12 scenarios ($p < 0.05$), suggesting that a higher P_{ci} tends to co-occur with more stable longitudinal and lateral control. Only scenarios 3 exhibited non-significant correlations ($p > 0.05$); the full results are

Table 8
Results of flow velocity.

Scenarios		V_i
Right turn, large radius	Ordinary	1.209
	Prototype	1.441
Left turn, large radius	Ordinary	0.594
	Prototype	0.653
Right turn, small radius	Ordinary	0.622
	Prototype	0.628
Left turn, small radius	Ordinary	0.582
	Prototype	0.645

provided in the Appendix B (Table B2).

To evaluate the dynamic stability of driving state under different environment designs, the autocorrelation function (ACF) and partial autocorrelation function (PACF) of the P_c time series were computed for each condition. A 95% confidence band was used as the significance threshold ($|\mathrm{ACF}| > 0.149$), and the results are presented in Fig. 16. Overall, the prototype design exhibited better medium- and long-term stability, and the long-lag correlations remained positive particularly in right-turn scenarios, indicating that it is more conducive to improving drivers' adaptation to spiral-tunnel environments. Short-term stability was mainly influenced by radius and direction: the 500 m condition showed the highest level (≈0.709), followed by 250 m (≈0.700), while 970 m was the lowest.

4.2.6. *Path analysis for prototype design*

The calculated path coefficients under the prototype design condition are shown in Fig. 17, and the corresponding validation results are provided in Appendix A, Table A1. Overall, the path analysis was basically able to characterize the parameterized relationships between environmental semantics and the composite VPF index. Specifically, among the four environmental semantic categories, M_{i1} and M_{i2} made the largest contributions, whereas M_{i3} and M_{i4} showed relatively weaker effects. The results indicate that M_{i1} exerted promoting effects on both velocity and cognitive resistance, while M_{i2} promoted velocity but inhibited cognitive resistance. Meanwhile, the hypothesized parametric relationship from V_i to F_i was relatively weak, suggesting that a certain relationship may exist between velocity and resistance, but it was not dominant.

5. Discussion

5.1. *Considering environmental information in driving cognition research*

The core motivation for applying SER theory in this study is to investigate the interaction between drivers and the environmental information they perceive. Accordingly, in scenario development we adopted SER principles and implemented a large-radius prototype with a sparser distribution of retroreflective rings, fewer traffic signs, and a more visually uniform overall environment. The equivalent-information-mass results showed (Fig. 9) reduced semantic areas for visual guidance facilities (M_{i1}) traffic signs (M_{i2}), and overall environment elements (M_{i3}). Because the prototype design assigned higher subjective weights to the first two semantic categories (M_{i1} and M_{i2}), the resulting equivalent quality increased. Moreover, since the total semantic area and total subjective weights are normalized and remain constant ($\sum \rho_{ij} = 1, \sum g_j = 1$), reducing some semantic categories necessarily increases the relative salience of others. Consequently, although the roadway semantics (M_{i4}) did not fundamentally change in content, its value increased numerically due to this trade-off. Similarly, in the small-radius prototype, denser retroreflective rings and signs, together with yellow lane lines and edge markings, increased the semantic area of visual guidance facilities (M_{i1}) and traffic signs (M_{i2}). Because visual guidance facilities and the roadway received higher subjective weights, the computed results in Fig. 10 exhibited corresponding increases. This evidence aligns with Ren et al. (2024) and supports the view that representing traffic scenes through

Table 9
Results of cognitive resistance.

Scenarios		F_i
Right turn, large radius	Ordinary	0.920
	Prototype	0.941
Left turn, large radius	Ordinary	0.790
	Prototype	0.565
Right turn, small radius	Ordinary	0.732
	Prototype	0.935
Left turn, small radius	Ordinary	0.707
	Prototype	0.640

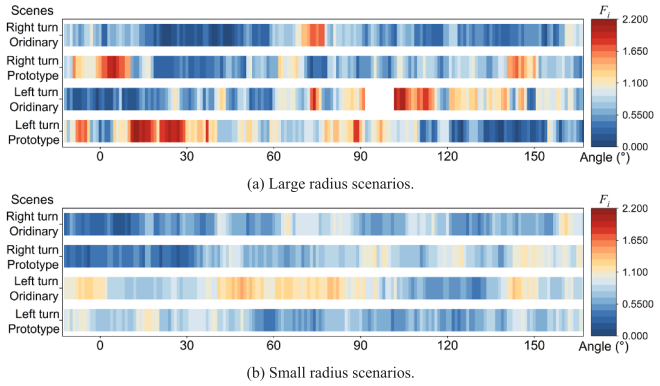

(a) Large radius scenarios.

(b) Small radius scenarios.

Fig. 12. Results of driver's cognitive load from different angles.

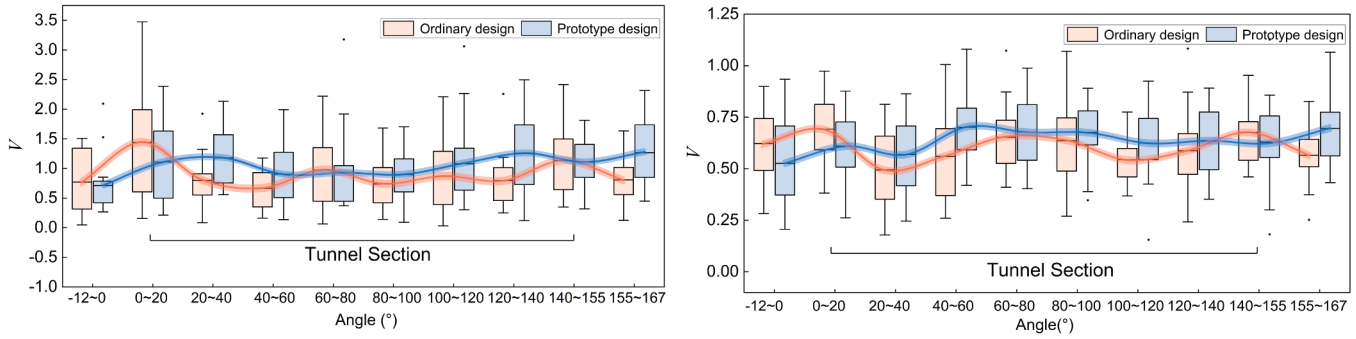

(a) Large radius scenarios.

(b) Small radius scenarios.

Fig. 11. Saccade amplitude results at different angles.

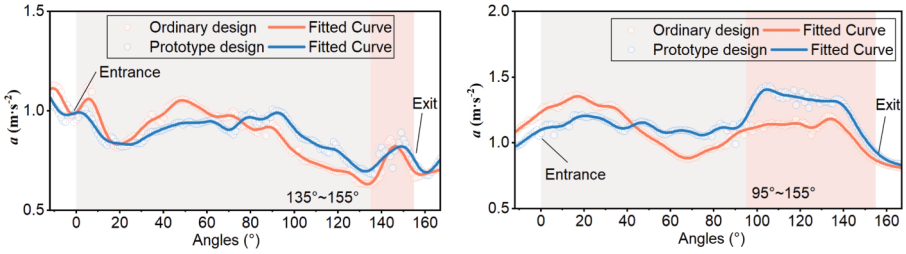

(a) Large radius scenes. (b) Small radius scenes.

Fig. 13. Acceleration results of driving under different working conditions.

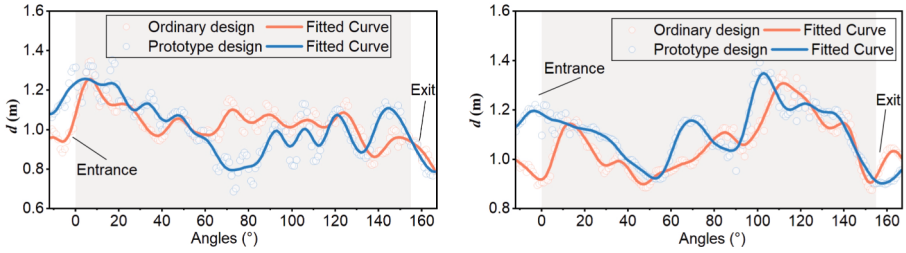

(a) Large radius scenarios. (b) Small radius scenarios.

Fig. 14. Trajectory deviation results of driving under different working conditions.

Table 10
Results of effective visual-perception capability P_{ci}.

Scenarios		P_{ci}
Right turn, large radius	Ordinary	48.2
	Prototype	51.7
Left turn, large radius	Ordinary	37.8
	Prototype	37.2
Right turn, small radius	Ordinary	39.5
	Prototype	41.9
Left turn, small radius	Ordinary	38.1
	Prototype	40.5

environmental semantics is an effective pathway for quantifying and evaluating road environments. Additionally, the substantial left–right difference of M_{ij} may be explained by direction-dependent visual exposure. The integration of environmental semantic segmentation provides data-level support for investigating driver visual perception.

Path analysis under the prototype design also offers an initial parameterized association between environmental semantics and cognition. Specifically, M_{i1} showed the largest total indirect effect on the P_{ci}, indicating that visual guidance facilities contributed more directly and consistently to cognitive improvement. Therefore, in the environmental optimization of spiral tunnels, priority should be given to improving the layout quality and saliency of two key facility categories, namely visual guidance facilities ($\alpha_1 = 0.058, \gamma_1 = 0.052$) and traffic signs ($\alpha_2 = 0.018, \gamma_2 = -0.031$). By enhancing the visibility, continuity, and recognizability of critical semantic information, drivers' visual perception and road understanding can be further improved. Meanwhile, the V_i to F_i path was weak (I = −0.0165), whereas the effects of V_i and F_i on P_{ci} were clearer. Wang et al. (2025a) reported that environmental design factors substantially influence driving behavior and cognitive load in spiral tunnels. When semantic information in the environment becomes more abundant or complex, visual search amplitude typically increases, drivers scan more frequently to search for and repeatedly confirm information, and cognitive load rises accordingly (Yang et al., 2025). However, SER theory emphasizes that good road design should enable drivers to understand the situation and make decisions naturally. This implies that evaluating driving task difficulty solely by visual search quantity or cognitive load is inherently partial and may overlook the role of well-structured environmental cues in supporting efficient cognition and action.

5.2. *Evaluating benefits of prototype design to visual-perception capability*

Neurophysiological evidence indicates that once environmental semantics are acquired through vision and enter drivers' cortical processing, the neural resources recruited during driving resemble those used to process linguistic information, confirming that understanding environmental semantics consumes cognitive resources (Xia et al., 2023). We found that the benefits of the prototype design were concentrated in the internal and exit section. Outside these locations, the environment design did not vary markedly with turning angle. Tunnel portals often constitute points of abrupt information input and oscillatory changes (Du et al., 2014), which are more likely to trigger shifts in cognitive state; therefore, they provide a sensitive window for revealing differences in environment design quality.

From the perspective of the visual pathway, the prototype design produced larger saccade amplitudes than the ordinary design under both large- and small-radius conditions. Notably, in both scenarios, saccade amplitude became more stably elevated after the tunnel entrance, suggesting that the prototype design helped drivers maintain a more continuous and active visual scanning state once they entered the spiral tunnel environment. In the large-radius condition, this pattern may indicate that the optimized design facilitated broader visual exploration by providing clearer and more interpretable environmental cues. In the small-radius condition, despite the stronger geometric constraint imposed by a tighter curve (Han et al., 2024), the prototype design still supported sustained scanning rather than restricting eye movements to a narrow local range. This implies that the prototype environment may have improved the organization and readability of visual information, thereby promoting more effective information uptake. Consistent with this interpretation, the computed composite VPF index remained higher under the prototype design, indicating that the increased saccade amplitude reflected enhanced visual-perception support rather than excessive or disorganized searching. Combining flow velocity and resistance within the VPF framework helps capture the balance between

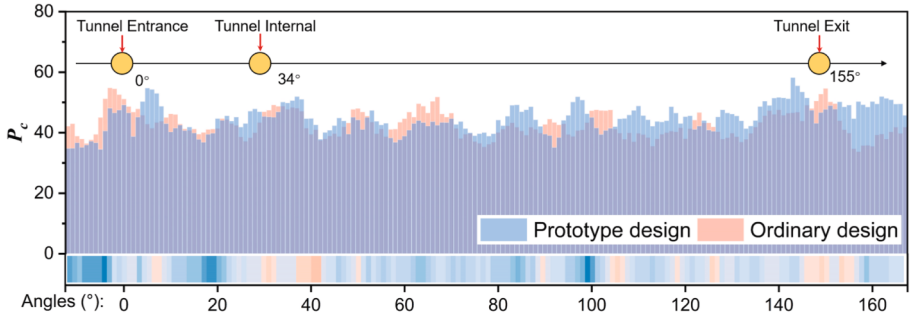

(a) Large radius scenes.

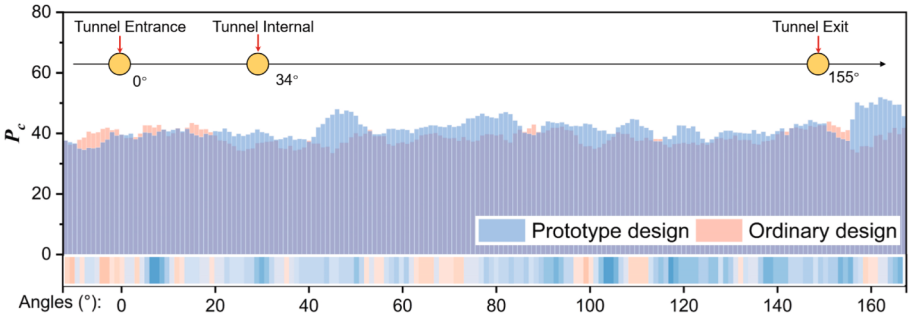

(b) Small radius scenes.

Fig. 15. Calculation results of effective visual perception capability under different conditions.

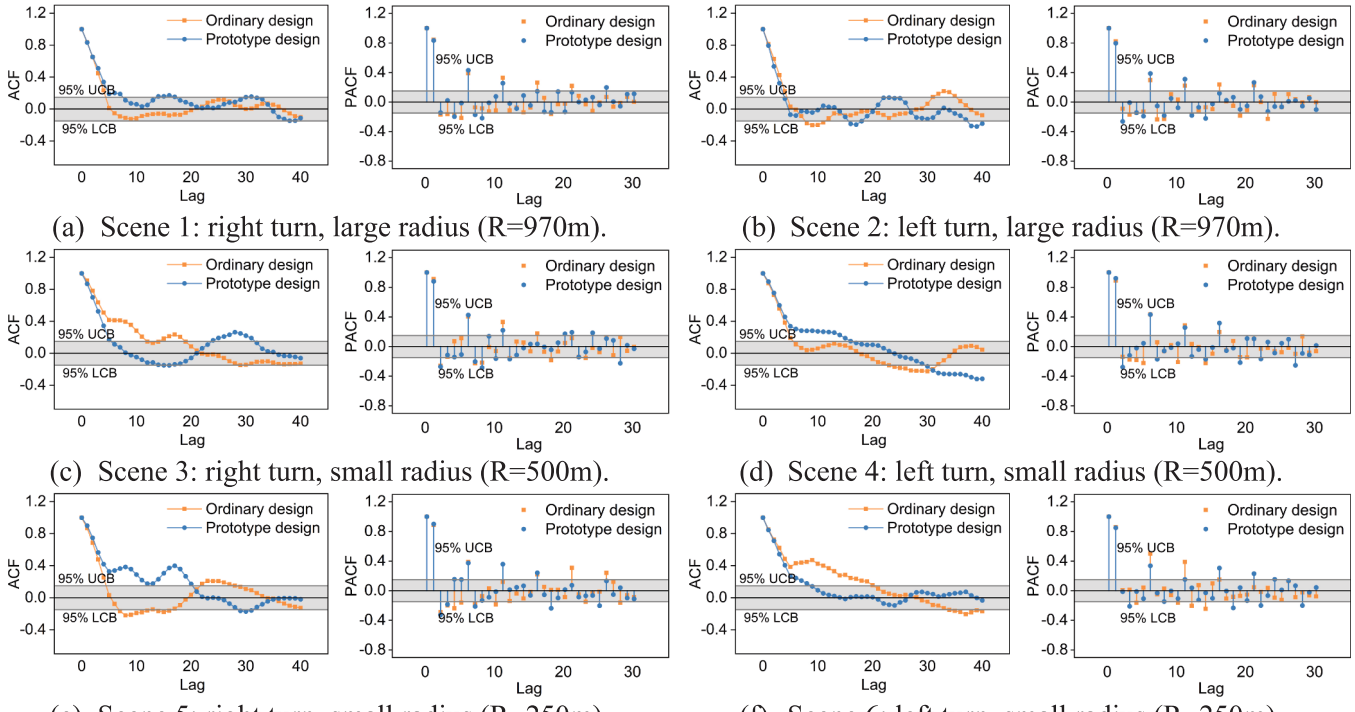

(a) Scene 1: right turn, large radius (R=970m). (b) Scene 2: left turn, large radius (R=970m).

(c) Scene 3: right turn, small radius (R=500m). (d) Scene 4: left turn, small radius (R=500m).

(e) Scene 5: right turn, small radius (R=250m). (f) Scene 6: left turn, small radius (R=250m).

Fig. 16. Calculation results of ACF and PACF under different conditions.

visual exploration and cognitive workload. Under the prototype design, saccade amplitude was generally higher after the tunnel entrance, whereas cognitive load did not increase accordingly in several key segments. This suggests more efficient visual information acquisition and helps explain the higher composite VPF index under the prototype design.

5.3. *Behavioral performance and visual-perception capability*

The results showed consistent trends between changes in visual-perception capability and the stability of speed control and trajectory keeping. Near the tunnel exit (155°), acceleration under the road prototype was consistently lower than that under the ordinary design, indicating more stable speed regulation at this critical segment. In large

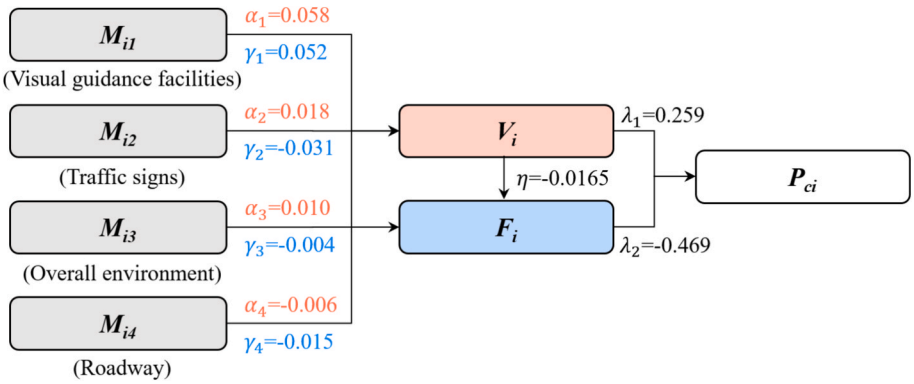

Fig. 17. Coefficients of path analysis.

radius cases, the road prototype design also reduced lateral deviation near the tunnel entrance, suggesting improved lane-keeping stability during the initial adaptation to the tunnel environment. Notably, as radius decreased, drivers tended to start reducing acceleration closer to the exit, implying that they increasingly adopted a stabilizing strategy near the portal rather than frequent speed fluctuations. Visual-perception capability triggering is not limited to binary decisions; it also involves shifts in task strategy and attentional allocation. When environmental demands increase abruptly and instantaneous cognitive requirements surge, drivers initiate compensatory behaviors. For example, Zhang et al. (2025) reported that under overly time-pressured conditions, drivers may make preliminary decisions before forming sufficient situation understanding. This evidence suggests that once visual-perception capability exceeds a critical threshold, the brain tends to trigger actions earlier to safeguard safety or efficiency.

From an engineering application perspective, these results indicate that the design of spiral tunnel environments should not adopt a unified configuration, but should implement differentiated design based on the driving task requirements under different radius conditions. For relatively wide and gentle large radius scenarios, stable operation should be supported by moderately simplifying the environment and maintaining clear key guidance information; For more constrained small radius scenarios, visual guidance and road boundary cues should be strengthened to help drivers form more cautious and clear path expectations. In addition, the entrance, the onset of stable turning, and the exit sections are more sensitive to cognitive changes and control fluctuations, and therefore can be prioritized for facility optimization and existing tunnel renovation.

6. Conclusion

As mountainous transportation infrastructure expands, spiral tunnels are increasingly used in highways across complex terrains. However, their distinctive geometry often induces spatial-cognitive difficulties that compromise driving safety, and existing studies still lack a system-level understanding of how integrated environment design shapes drivers' cognition. Based on SER theory, we develop a road prototype design method for the overall visual environment design of spiral tunnels and establish a visual- perception fluid (VPF) model enabled by environmental semantic segmentation to quantify drivers' visual-perception performance in spiral tunnels. The main conclusions are:

The results show that the VPF model can serve as an effective tool for evaluating whether the road environment is conducive to efficient visual perception. Based on environmental semantic segmentation, the model demonstrates the feasibility of transforming facility design from qualitative description into computable variables. The results show that the prototype design consistently increases the equivalent mass of M_{i1} (visual guidance facilities) and M_{i4} (roadway) across almost all conditions. Combined with its concurrent criterion-related validity with driving behavior, these findings indicate the potential value of the VPF model for evaluating the effects of facility optimization.

The proposed prototype design improves the visual environment of spiral tunnels in most scenarios. Relative to the ordinary design, the overall visual-perception capability increased by 1.9 (4.6%), with gains of 1.1 (3.3%) for the large-radius group and 2.4 (6.2%) for the small-radius group. Stratified paired permutation tests confirmed statistically significant improvements ($p < 0.05$). The road prototype design developed in this study can provide a methodological framework for the systematic environmental design of spiral tunnels, and may provide practical guidance for environmental optimization in spiral tunnels with similar scales and comparable operational demands.

Simultaneously, the improvement in visual-perception performance brought by the road prototype design in spiral tunnels was mainly concentrated in the middle and exit sections. Autocorrelation function (ACF) analysis further showed stronger medium- and long-term stability in these sections ($|\mathrm{ACF}| > 0.149$), indicating better environmental adaptability and greater behavioral stability of drivers in the mid-to-late segments. This result suggests that the entrance section should be treated as a priority intervention zone, while the middle and exit sections should be regarded as key locations for the continued optimization of visual guidance and operational stability.

The numerical results of the path analysis showed that visual guidance facilities ($\alpha_1 = 0.058, \gamma_1 = 0.052$) and traffic signs ($\alpha_2 = 0.018, \gamma_2 = -0.031$) were the two semantic categories with relatively greater effects on visual perception, acting through the pathways of visual information acquisition and attentional resource consumption. Therefore, in the design of spiral-tunnel environments, priority may be given to visual-guidance signs and traffic signs, with optimization focused on their placement density and salience.

This study extends the application boundary of SER theory by adapting it to spiral tunnels as a cognitively complex driving context, thereby addressing the limitation of prior SER research that focuses mainly on ordinary road scenarios. It also proposes an interdisciplinary framework that integrates traffic-environment representation, cognitive mechanisms, and multi-criteria evaluation, bridging transportation engineering and cognitive psychology and enriching the theoretical basis for road-environment design in complex terrains. Moreover, the proposed optimization strategy helps to consider the balance between construction cost and operational safety, providing a design framework for spiral tunnels with different radii, thus offering practical engineering value.

Despite these contributions, the simulator-based platform still differs from real-world conditions. It should be noted that the VPF model currently focuses on information sampling and resource loss at the level of visual perception, and direct evidence linking it to underlying neural mechanisms remains limited. It is also more suitable for relative comparisons across alternatives within the same tunnel type or design system, where semantic categories and segmentation outputs are more

consistent. Moreover, special traffic conditions (e.g., congestion, overtaking occasion or unexpected events) may substantially alter information demand and attention allocation, which should be examined in future work. Future work will conduct field experiments in real spiral tunnels with different geometric shapes, and will develop and train a tunnel-specific semantic segmentation model using in-situ driving-environment images to further calibrate prototype design parameters. Furthermore, we will also test causal pathways using mixed-effects of driver behaviors with larger samples and more scenarios, thereby improving generalizability and engineering implementability.

CRediT authorship contribution statement

Yanzi Xia: Writing – review & editing, Writing – original draft, Methodology, Conceptualization. **Chi Zhang:** Writing – review & editing, Writing – original draft, Supervision, Funding acquisition, Conceptualization. **Min Zhang:** Validation, Supervision, Investigation, Formal analysis, Conceptualization. **Bo Wang:** Writing – review & editing, Validation, Data curation. **Yanyang Gao:** Validation, Software. **Sheng Xu:** Software, Data curation.

Declaration of competing interest

The authors declare that they have no known competing financial interests or personal relationships that could have appeared to influence the work reported in this paper.

Acknowledgements

This work was supported by the National Natural Science Foundation of China (grant number 72371036); Shaanxi Provincial Social Science Fund Project (grant number 2025R018); Fundamental Research Funds for the Central Universities (grant number CHD 300102215206); and the Science and Technology Project of Sichuan Transportation Department (grant number 2023-A-04).

Appendix A. Path model

The path model was formulated as follows:

$$V_i = \alpha_0 + \sum_{j=1}^{4} \alpha_j M_{ij} + \varepsilon_{V_i} \tag{A1}$$

where V_i is the velocity indicator for sample i, M_{ij} is the j^{th} environmental semantic indicator, α_0 is the intercept, α_j are path coefficients, and ε_{V_i} is the residual term.

$$F_i = \gamma_0 + \sum_{j=1}^{4} \gamma_j M_{ij} + \eta V_i + \varepsilon_{F_i} \tag{A2}$$

where F_i is the cognitive resistance indicator for sample i, γ_0 is the intercept, γ_j are path coefficients from the semantic indicators to F_i, η is the coefficient from V_i to F_i, and ε_{F_i} is the residual term.

$$P_{ci} = \beta_0 + \lambda_1 V_i - \lambda_2 F_i + \varepsilon_{P_i} \tag{A3}$$

where P_{ci} is the VPF index, β_0 is the intercept, λ_1 and λ_2 are path coefficients, and ε_{P_i} is the residual term.

For the j^{th} environmental semantic indicator, the indirect effect through the first mediator V_i was calculated as:

$$I_{Vj} = \alpha_j \lambda_1 \tag{A4}$$

The indirect effect through the mediator F_i was calculated as:

$$I_{Fj} = -\gamma_j \lambda_2 \tag{A5}$$

The sequential indirect effect through the path M_{ij} to P_{ci} was calculated as:

$$I_{V \to Fj} = -\alpha_j \eta \lambda_2 \tag{A6}$$

Accordingly, the total indirect effect of the j^{th} environmental semantic indicator was expressed as:

$$I_j = \alpha_j \lambda_1 - \gamma_j \lambda_1 - \alpha_j \eta \lambda_2 \tag{A7}$$

Table A1
Bootstrap 95% confidence intervals for the indirect effects of environmental information.

Semantic class	I_{Vj}	95% CI		I_{Fj}	95% CI		I_j	95% CI	
Visual guidance facilities	0.017	−0.048	0.091	0.026	−0.097	0.151	0.043	−0.101	0.189
Traffic signs	0.014	−0.033	0.067	−0.013	−0.091	0.060	0.002	−0.083	0.096
Overall environment	0.003	−0.118	0.129	0.007	−0.202	0.213	0.010	−0.236	0.261
Roadway	0.001	−0.096	0.103	−0.001	−0.168	0.167	0.002	−0.195	0.204

Appendix B

Table B1
Retroreflective ring spacing for different visible ring counts under varying radius and curve directions (m).

Direction	Radius (m)	1 visible ring	2 visible rings	3 visible rings	4 visible rings
Right turn	250	111.4	55.7	37.1	27.8
	500	162.7	81.4	54.2	40.7
	970	231.5	115.8	77.2	57.9
Left turn	250	93.3	46.7	31.1	23.3
	500	138.1	69.1	46.0	34.5
	970	197.9	99.0	66.0	49.5

Table B2
Spearman's rank correlations between P_{ci} and driving behaviors (Bonferroni-corrected).

Index of scenarios	Acceleration		Lateral deviation	
	r	p	r	p
1	−0.276	*	−0.237	*
2	−0.148	***	0.141	***
3	0.277	0.284	−0.284	0.102
4	−0.070	*	−0.107	**
5	−0.154	***	0.109	***
6	−0.256	*	−0.257	**
7	0.128	**	−0.174	**
8	−0.176	**	−0.206	**
9	−0.178	**	0.180	**
10	−0.179	***	−0.181	***
11	−0.468	***	−0.397	**
12	−0.612	***	−0.537	***

Data availability

The authors do not have permission to share data.

References

Alyan, E., Reiser, J.E., Wascher, E., 2026. Real-time monitoring of driver cognitive states: linking driving behavior to neural oscillations. Transport. Res. F: Traffic Psychol. Behav. 116, 103423. https://doi.org/10.1016/j.trf.2025.103423.

Boender, J., 2014. Self-explaining roads in the netherlands, in: Rural Roads Design, Meeting No. 5, April 3–4, 2014. NMFV / CROW, Den Sorte Diamant, The Royal Library, Copenhagen, Denmark.

Chen, B., Zhao, X., Li, Y., Liu, X., 2025. Mapping the knowledge domain of crash risk in older drivers studies: a scientometric analysis. J. Traffic Transp. Eng. Engl. Ed. 12 (3), 587–602. https://doi.org/10.1016/j.jtte.2024.05.002.

Cheng, B., Misra, I., Schwing, A.G., Kirillov, A., Girdhar, R., 2021. Masked-attention mask transformer for universal image segmentation. Proceedings of IEEE/CVF Conference on Computer Vision and Pattern Recognition (CVPR).

Du, Z., Han, L., Mei, J., He, S., Yang, Y., 2023. Optimization research framework of visual environment for small radius highway long tunnel based on mental rotation effect. J. Tongji Univ. Sci. 51 (9), 1372–1382. https://doi.org/10.11908/j.issn.0253-374x.23221.

Du, Z., Wang, S., Yang, L., Jiao, F., 2021. Experimental study on the efficacy of retroreflective rings in the curved freeways tunnels. Tunn. Undergr. Space Technol. 110, 103813. https://doi.org/10.1016/j.tust.2021.103813.

Faidah, U.N., Maulana, I., Efranto, R.Y., 2026. Driver mental workload measurement trends and cognitive impacts: a literature review. Theor. Issues Ergon. Sci. 1–16. https://doi.org/10.1080/1463922X.2025.2608063.

Greaves, H., 2013. Epistemic decision theory. Mind 122 (488), 915–952. https://doi.org/10.1093/mind/fzt090.

Han, L., Du, Z., Wang, S., 2025a. The impact of spiral tunnel characteristics on driver HRV and stress perception: a naturalistic driving experiment. Accid. Anal. Prev. 214, 107983. https://doi.org/10.1016/j.aap.2025.107983.

Han, L., Du, Z., Wang, S., 2025b. Exploring drivers' psychological responses in spiral tunnel: visual attention and subjective perceptions. Traffic Inj. Prev. 26 (7), 775–784. https://doi.org/10.1080/15389588.2025.2459860.

Han, L., Du, Z., Wang, S., He, S., 2024. The effects of tunnel radius, turn direction, and zone characteristics on drivers' visual performance. Tunn. Undergr. Space Technol. 152, 105912. https://doi.org/10.1016/j.tust.2024.105912.

Han, L., Zhou, H., Gu, P., Du, Z., 2025c. Spiral tunnel driving and cognitive load: an eye-tracking investigation into tunnel geometry and traversal effects. Traffic Inj. Prev. 1–12. https://doi.org/10.1080/15389588.2025.2561772.

He, S., Liang, B., Pan, G., Wang, F., Cui, L., 2017. Influence of dynamic highway tunnel lighting environment on driving safety based on eye movement parameters of the driver. Tunn. Undergr. Space Technol. 67, 52–60. https://doi.org/10.1016/j.tust.2017.04.020.

Iida, H., Nakagawa, T., Spoerer, K., 2012. Game information dynamic models based on fluid mechanics. Entertain. Comput. 3 (3), 89–99. https://doi.org/10.1016/j.entcom.2012.04.002.

Jiao, F., Du, Z., Wong, Y.D., He, S., Xu, F., Zheng, H., 2022. Self-explaining performance of visual guiding facilities in urban road tunnels based on speed perception. Tunn. Undergr. Space Technol. 122, 104371. https://doi.org/10.1016/j.tust.2022.104371.

Jiao, F., Du, Z., Wong, Y.D., Mei, J., Sun, F., 2023. Design and evaluation of visual guiding facilities along urban road tunnel horizontal curves based on vision and speed perception. Tunn. Undergr. Space Technol. Incorporating Trenchless Technol. Res. 133, 104937. https://doi.org/10.1016/j.tust.2022.104937.

Kanaan, D., Powell, M., Lu, M., Donmez, B., 2024. In-vehicle displays for driving automation: a scoping review of display design and evaluation using driver gaze measures. Transp. Rev. 44 (4), 858–888. https://doi.org/10.1080/01441647.2024.2336921.

Kircher, K., Ahlstrom, C., 2012. The impact of tunnel design and lighting on the performance of attentive and visually distracted drivers. Accid. Anal. Prev. 47, 153–161. https://doi.org/10.1016/j.aap.2012.01.019.

Kujala, T., Kircher, K., Ahlström, C., 2023. A review of occlusion as a tool to assess attentional demand in driving. Hum. Factors 65 (5), 792–808. https://doi.org/10.1177/00187208211010953.

Li, M., Feng, Z., Zhang, W., Wang, L., Wei, L., Wang, C., 2023. How much situation awareness does the driver have when driving autonomously? A study based on driver attention allocation. Transp. Res. Part C Emerg. Technol. 156, 104324. https://doi.org/10.1016/j.trc.2023.104324.

Lindenberg, S., 2018. How cues in the environment affect normative behaviour, in: Steg, L., Groot, J.I.M. (Eds.), Environmental Psychology. Wiley, pp. 144–153. doi: 10.1002/9781119241072.ch15.

Liu, J.-C., Li, K.-A., Yeh, S.-L., Chien, S.-Y., 2022. Assessing perceptual load and cognitive load by fixation-related information of eye movements. Sensors 22 (3), 1187. https://doi.org/10.3390/s22031187.

Parham, A.H., Womack, K.N., Hawkins, H.G., 2003. Driver understanding of pavement marking colors and patterns. Transp. Res. Rec. 1844 (1), 35–44. https://doi.org/10.3141/1844-05.

Rabinovich, M.I., Afraimovich, V.S., Bick, C., Varona, P., 2012. Information flow dynamics in the brain. Phys. Life Rev. 9 (1), 51–73. https://doi.org/10.1016/j.plrev.2011.11.002.

Raza, M.S., Murtaza, M., Cheng, C.T., Muslam, M.M.A., Albahlal, B.M., 2024. Systematic review of cognitive impairment in drivers through mental workload using physiological measures of heart rate variability. Front. Comput. Neurosci. 18. https://doi.org/10.3389/fncom.2024.1475530.

Ren, R., Xiao, Z., Wang, Y., Song, X., 2025. Driving safety of low-position lighting in highway tunnels based on visual performance. J. Traffic Transp. Eng. Engl. Ed. 12 (3), 616–638. https://doi.org/10.1016/j.jtte.2025.05.001.

Ren, W., Yu, B., Chen, Y., Gao, K., Bao, S., Wang, Z., Qin, Y., 2024. An intelligent optimization method for the facility environment on rural roads. Comput. Aided Civ. Inf. Eng. 39 17, 2559–2580. https://doi.org/10.1111/mice.13209.

Rose, E.R., Carlson, P.J., 2005. Spacing chevrons on horizontal curves. Transp. Res Rec.: J. Transp. Res. Board 1918, 84–91. https://doi.org/10.3141/1918-11.

Sayood, K., 2018. Information theory and cognition: a review. Entropy 20 (9), 706. https://doi.org/10.3390/e20090706.

Song, Y., Zhu, H., Shen, Y., Feng, S., 2024. Green tunnel lighting environment: a systematic review on energy saving, visual comfort and low carbon. Tunn. Undergr. Space Technol. 144, 105535. https://doi.org/10.1016/j.tust.2023.105535.

Souza, A., Freitas, D., 2022. Towards the improvement of the cognitive process of the synthesized speech of mathematical expression in MathML: an eye-tracking. In: In: Proceedings of the 2022 International Conference on Interactive Media, Smart Systems and Emerging Technologies (IMET), pp. 1–8. https://doi.org/10.1109/IMET54801.2022.9929541.

Specifications for Highway Geometric Design, 2017. Ministry of Transport of the People's Republic of China, Beijing, China.

Steelman, K.S., McCarley, J.S., Wickens, C.D., 2017. Theory-based models of attention in visual workspaces. Int. J. Human-Computer Interact. 33 (1), 35–43. https://doi.org/10.1080/10447318.2016.1232228.

Talebpour, A., Zhang, Y., Radvand, T., Yousefi, M., 2024. Advancing self-enforcing streets phase 1: The relationship between roadway environment and crash severity (No. FHWA-ICT-24-023). University of Illinois Urbana-Champaign, Illinois Center for Transportation, Urbana, IL, USA.

Theeuwes, J., 2021. Self-explaining roads: what does visual cognition tell us about designing safer roads? Cogn. Res. Princ. Implic. 6 (1), 15. https://doi.org/10.1186/s41235-021-00281-6.

Theeuwes, J., Snell, J., Koning, T., Bucker, B., 2024. Self-explaining roads: Effects of road design on speed choice. Transp. Res. Part F Traffic Psychol. Behav. 102, 335–361. https://doi.org/10.1016/j.trf.2024.03.007.

Theeuwes, J., 2025. Attentional capture and control. Annu. Rev. Psychol. 76, 251–273. https://doi.org/10.1146/annurev-psych-011624-025340.

Van der Horst, R., Kaptein, N., 1998. Self-explaining roads, in: Proceedings of the 11th Workshop of the ICTCT (International Cooperation on Theories and Concepts in Traffic Safety). Presented at the ICTCT, Budapest, Hungary, pp. 15–32.

Wang, R., Wang, Y., Xu, X., Pan, X., 2020. Mechanical thoughts and applications in cognitive neuroscience. Adv. Mech. 50 (1), 202012. https://doi.org/10.6052/1000-0992-20-008.

Wang, S., Han, L., Du, Z., He, S., Zheng, H., Yang, L., Jiao, F., 2025a. Can retroreflective rings enhance drivers' safety perception of spatial right-of-way in freeway tunnels? A simulation exploration. Accid. Anal. Prev. 209, 107825. https://doi.org/10.1016/j.aap.2024.107825.

Wang, T., Ge, Y.-E., Wang, Y., Chen, W., Fu, Q., Niu, Y., 2024. A novel model for real-time risk evaluation of vehicle–pedestrian interactions at intersections. Accid. Anal. Prev. 206, 107727. https://doi.org/10.1016/j.aap.2024.107727.

Wang, Y., Kang, X., Wang, X., Yang, Y., Li, X., 2025b. High-dynamic impact mechanism of complex spiral tunnel environments on driving behavior based on multi-source data fusion. Tunn. Undergr. Space Technol. 161, 106584. https://doi.org/10.1016/j.tust.2025.106584.

Wickens, C.D., 2015. Noticing events in the visual workplace: The SEEV and NSEEV models, in: The Cambridge Handbook of Applied Perception Research, Vol. II, Cambridge Handbooks in Psychology. Cambridge University Press, New York, NY, US, pp. 749–768. doi:10.1017/CBO9780511973017.046.

Wolfe, B., Sawyer, B.D., Rosenholtz, R., 2022. Toward a theory of visual information acquisition in driving. Hum. Factors 64 (4), 694–713. https://doi.org/10.1177/0018720820939693.

Xia, Y., Geng, M., Chen, Y., Sun, S., Liao, C., Zhu, Z., Li, Z., Ochieng, W.Y., Angeloudis, P., Elhajj, M., Zhang, L., Zeng, Z., Zhang, B., Gao, Z., Chen, X. (Michael), 2023. Understanding common human driving semantics for autonomous vehicles. Patterns 4 (7), 100730. https://doi.org/10.1016/j.patter.2023.100730.

Xia, Y., Zhang, C., Zhang, M., Zhang, H., Wang, B., 2025. Characterizing the driving cognition within spiral tunnels based on SER principle. Tunn. Undergr. Space Technol. 163, 106649. https://doi.org/10.1016/j.tust.2025.106649.

Xing, G., Ma, Y., Chen, S., Xing, Y., Pang, Q., Gao, L., 2025a. Investigating the self-explaining performance of visual guidance facilities in extra-long spiral tunnels based on drivers' spatial perception and visual attention distribution. Accid. Anal. Prev. 217, 108040. https://doi.org/10.1016/j.aap.2025.108040.

Xing, G., Ma, Y., Chen, S., Xing, Y., Zhang, C., 2025b. Exploring the impact zone at spiral tunnel entrances and exits: Analyzing the vehicle control process from invalidation to recovery under environmental perturbations. Accid. Anal. Prev. 217, 108046. https://doi.org/10.1016/j.aap.2025.108046.

Xing, G., Ma, Y., Chen, S., Zhang, J., Xing, Y., 2025c. Invalidation and adaptation of vehicle control under environmental perturbations in spiral tunnels: effects of alignment radii and perturbation locations. Tunn. Undergr. Space Technol. 162, 106661. https://doi.org/10.1016/j.tust.2025.106661.

Xinhua News Agency, 2022. Ministry of public security releases 2021 national motor vehicle and driver data [WWW Document]. Minist. Public Secur. Releases 2021 Natl. Mot. Veh. Driv. Data. URL https://www.gov.cn/xinwen/2022-01/11/content_5667669.htm (accessed 11.26.24).

Yan, Y., Zhang, Y., Yuan, H., Wan, L., Ding, H., 2024. Safety effect of tunnel environment self-explaining design based on situation awareness. Tunn. Undergr. Space Technol. 143, 105486. https://doi.org/10.1016/j.tust.2023.105486.

Yang, G., 2025. Cognitive Gravity and Its Singularity: A Unified Physics of Expert Cognitive Inertia and Organizational Adaptive Inertia. doi:10.2139/ssrn.5376502.

Yang, Y., Wu, X., Yin, D., Easa, S.M., Zheng, X., 2025. Effect of traffic sign's information supply speed on driver performance at tunnel entrances. Transp. Res. Part F Traffic Psychol. Behav. 111, 217–237. https://doi.org/10.1016/j.trf.2025.03.005.

Ye, Y., He, J., Hu, J., Sun, S., Zhang, C., Yan, X., Wang, C., Qin, P., 2025. Exploring the effect of driving environment on driver stress: a framework based on urban street view and explainable machine learning. J. Intell. Transp. Syst. 1–17. https://doi.org/10.1080/15472450.2025.2478475.

Zeng, Q., Chen, Y., Zheng, X., He, S., Li, D., Nie, B., 2023. Optimization of underground cavern sign group layout using eye-tracking technology. Sustainability 15 (16), 12604. https://doi.org/10.3390/su151612604.

Zhang, C., Wang, B., Li, Y., Hou, L., Zhang, M., Liu, C., Xie, Z., 2022. Freeway traffic safety evaluation using virtual reality: focus on compound curve. Sustainability 14 (22), 15170. https://doi.org/10.3390/su142215170.

Zhang, Z., Wang, C., Luan, Z., Zhao, W., 2025. Evolution mechanism and progressive reshaping model of driving behaviors when humans take over intelligent vehicles. Commun. Eng. 4 (1), 181. https://doi.org/10.1038/s44172-025-00510-6.

Zheng, H., Du, Z., Jia, C., Zhu, L., He, S., Mei, J., 2025. Evaluating the effectiveness of rhythmic visual guidance technology for mitigating driving risks in highway tunnel groups: a simulation study. Accid. Anal. Prev. 212, 107940. https://doi.org/10.1016/j.aap.2025.107940.